*Kinetics and Catalysis, Vol. 42, No. 4, 2001, pp. 511–519. Translated from Kinetika i Kataliz, Vol. 42, No. 4, 2001, pp. 565–573.*


# Theoretical Study of the Catalytic Cycle for Ethylene Hydrogenation on a Dipalladium Cluster

**V. M. Mamaev *, I. P. Gloriozov *, Yu. V. Babin **, and E. V. Zernova ***

** Department of Chemistry, Moscow State University, Moscow, 119899 Russia*

*** Far East Academy of Economics and Management, Vladivostok, Russia*

Received July 5, 1999

**Abstract**—A theoretical study of the potential energy surface is carried out for the catalytic cycle of ethylene hydrogenation on a $Pd_2$ cluster using the reaction-path Hamiltonian. The catalytic cycle consists of five related reactions involving ten stationary points. The isomerization of the bridged $Pd_2H_2$ complex into the *trans* complex with a maximal barrier of 21.5 kcal/mol rather than the activation of the H–H bond is the most important reaction step. A conclusion is drawn that catalysts based on dipalladium complexes in which the dihydride product readily forms a *trans* form can be active in ethylene hydrogenation.

## INTRODUCTION

During the past 20 years, many papers have appeared that were devoted to quantum-chemical studies of catalytic reactions with organometallic compounds: olefin addition reactions [1–5], as well as oxidative addition and reductive elimination, including activation of H–H, C–H, and C–C bonds [6–18], which are important steps in hydrocarbon conversion. However, studies of the complete catalytic cycle with all its steps remain a hard problem to solve. The first theoretical study of homogeneous olefin hydrogenation on a rhodium complex was carried out by Morokuma and co-workers [19]. More recently, the same authors studied olefin hydroboration [20] and hydroformylation [21] on the same complex. In the theoretical study of alkene and alkyne hydroboration by diphosphine complexes of Pd and Pt [22, 23], they determined the reasons for $C_2H_4$ inactivity (a greater height of the activation barrier for hydrocarbon insertion into a Pt–B bond and endothermicity) and palladium complex inactivity in alkyne diboration (the impossibility of B–B oxidative addition to $Pd(PH_3)_2$ because of endothermicity and a small barrier for the reverse reaction: 0.1 kcal/mol). Albert *et al.* [24] studied the catalytic cycle of ethylene addition to phenyl bromide with the participation of a palladium complex with two diaminocarbene ligands. It was found that the key steps in the catalytic transformation are ethylene insertion into a palladium–phenyl bond and β-elimination (their activation barriers are 8.3 and 11.5 kcal/mol, respectively). The most comprehensive reviews of theoretical studies of catalytic reactions in the presence of transition metals are cited here in Ref. 25. All these studies include the calculation of stationary points for elementary steps by *ab initio* and DFT methods and then choosing the potential energy surface (PES) profile for the whole catalytic cycle.

The goal of this theoretical work was to study the catalytic hydrogenation of ethylene on a $Pd_2$ cluster, which is, in our opinion, a more promising catalyst compared with mononuclear complexes. Earlier [26], we studied in detail the oxidative addition of $H_2$ to a $Pd_2$ cluster based on the reaction-path Hamiltonian [27]. We showed that the potential energy surface has a complex shape with several valleys and stationary points. The global minimum is at the planar pseudosquare complex with energy of –34 kcal/mol with respect to separate reactants. This complex lies on a barrier-free reaction path. Another path passes through a bifurcation point (corresponding to a *cis*-product) and a transition state. It leads to a *trans*-product whose energy is 18 kcal/mol higher. In this work, we supplemented this reaction by the steps of ethane and ethylene formation

$$Pd_2 + H_2 \longrightarrow Pd_2H_2, \quad (1)$$

$$Pd_2H_2 + C_2H_4 \longrightarrow Pd_2 + C_2H_6. \quad (2)$$

## CALCULATION PROCEDURE

The quantum-chemical method applicable to the calculation of the potential energy surface for complex molecular systems with transition metals, which accommodates the reaction-path Hamiltonian approach, was CNDO/$S^2$ developed by G.M. Zhidomirov and co-workers [28, 29]. This method is rather efficient because it takes into account the nonorthogonality of basis orbitals by using a transform to the symmetrically-orthogonal basis. In this sense, CNDO/$S^2$ is analogous to SINDO-1 [30], but CNDO/$S^2$ uses an empirical parameter to correct the diagonal entry of the one-electron Hamiltonian matrix. CNDO/$S^2$ also uses the modified formula for the resonance integral, which connects two asymptotics—the interaction of two similar orbitals and the interaction of orbitals with radically different ionization potentials. In CNDO/$S^2$, one-center

0023-1584/01/4204-0511$25.00 

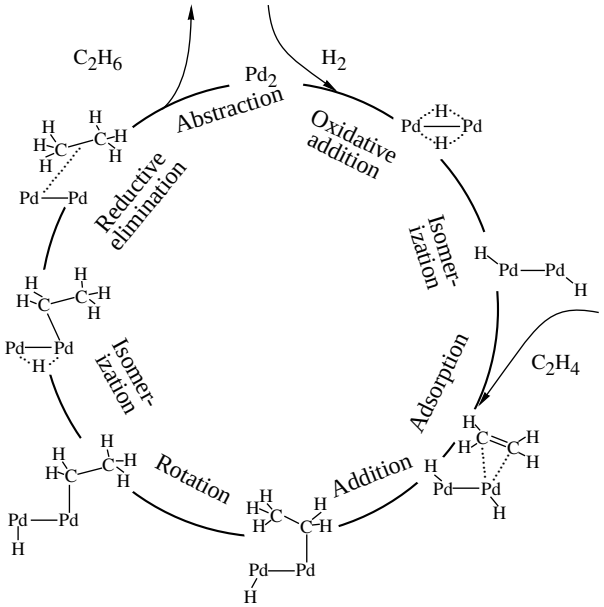


**Fig. 1.** Catalytic cycle of ethylene hydrogenation on the $Pd_2$ cluster.

two-electron integrals are introduced as parameters determined from atomic spectra. The exponents for atomic *d*-orbitals are determined from the condition of the best reproducibility for overlap integrals calculated from numeric Hartree–Fock functions. This justifies the use of one-exponent basis functions.

The above features make CNDO/S$^2$ capable of reproducing the characteristics of geometry and energy of molecular systems obtained in experiments or by high-level *ab initio* calculations taking into account correlation and relativistic correction. To calculate the elements of reaction-path Hamiltonian (RPH), we used a computer program developed by us earlier [31]. For the main stationary points on the potential energy surface of the catalytic cycle, we additionally carried out DFT calculations in two approximations for the exchange-correlation energy (DFT-BLYP [32, 33] and DFT-PBE [34]) incorporated in the program [35].

## RESULTS AND DISCUSSION

Detailed studies of potential energy surfaces for reactions (I) and (II) by the CNDO/S$^2$ method and RPH allowed us to isolate five related reaction paths: ($RP_1$–$RP_5$), which are elementary steps of the complete catalytic cycle. Figure 1 shows this cycle.

### *Oxidative Addition of $H_2$ to $Pd_2$ Cluster*

As mentioned above, $RP_1$ is a barrier-free path from separate reactants $H_2$ and $Pd_2$ to a bridging planar pseudosquare $Pd_2H_2$ complex (**I**) (Fig. 2). The reaction path is described (as in all further steps) in the form a normal coordinate *s* in Å (amu)$^{1/2}$, where amu is the atomic mass unit. That is, the mass of proton is taken as a unit mass, and the energy $\Delta E$ is relative to separate reactants. If *s* is between 4.5 and 5 Å (amu)$^{1/2}$, $RP_1$ has an area with a minimal gradient norm and an inflection point in this area. The vector of the reaction coordinate in the transition from the separate reagents to the inflection point involves mostly translation of unchanged $H_2$ and $Pd_2$ molecules toward each other. As this takes place, the H–H bond length increases to only 0.94 Å. Near the inflection point, the vibration $q$(H–H) transforms into the $q^+$(Pd–H) mode when the corresponding frequency $\omega_6$ decreases. Vibrational frequencies $\omega_3$–$\omega_6$ correspond to four vibrations of the $Pd_2H_2$ complex. Their symmetries are $A_1$, $A_2$, $B_1$, and $B_2$, respectively. The frequency $\omega_2$ refers to the $Q$(Pd–Pd) bond. The frequency $\omega_1$ corresponding to the reaction coordinate has an imaginary value of 500i cm$^{-1}$ (in Figs. 3–7, imaginary values are shown as negative). At $s > 4$ Å (amu)$^{1/2}$, the $RP_1$ vector virtually represents the internal rotation $\chi$(PdH–PdH). Along the whole length of $RP_1$ for the molecular system, the symmetry $C_{2v}$ is preserved. Reaction (I) was analyzed in detail earlier [26]. Further studies shows that an ethylene molecule cannot insert into a Pd–H bond of complex **I**. Rather, an adsorption complex is formed. The *cis*-complex is active enough to continue the catalytic cycle. DFT-BLYP calculations for complex **I** compare well to CNDO/S$^2$ calculation, whereas DFT-PBE approximation underestimates energy probably because of overestimating the exchange and correlation contributions to the bridged structure (Fig. 2).

### *Isomerization of the $Pd_2H_2$ Complex in the Presence of $C_2H_4$*

$RP_2$ corresponds to the transition from pseudosquare complex **I** to the *trans*-complex **II** in separate reactants $Pd_2H_2$ and $C_2H_4$ (see Fig. 3, which describes the frequencies of $Pd_2H_2$ and one additional frequency $\omega_{1a}$ due to the presence of $C_2H_4$). The $RP_2$ vector includes the shortening of the Pd–Pd distance and an increase in the plane Pd–Pd–H angles. This vector corresponds to the frequency $\omega_1$. Energy of the system increases by 17.3 kcal/mol with a barrier of 21.5 kcal/mol ($TS_1$). In the area of the reaction path with $s > 0$, frequencies $\omega_5$ and $\omega_6$ are the symmetric and asymmetric vibrations of Pd–H, $\omega_3$ and $\omega_4$ are the symmetric and asymmetric angular vibrations Pd–Pd–H. Saddle $TS_1$ has a second imaginary frequency $\omega_2$, which refers to the rotation of Pd–H bonds relatively to the Pd–Pd bond. Motion along the reaction path corresponding to rotation resulting in the *cis* product, which is higher in energy than the *trans*-product [26]. DFT calculation gives similar results for the structures of stationary points (Fig. 3). Note that they also give two imaginary frequencies for $TS_1$. When the DFT-BLYP method is used for the planar *trans*-product, there is no minimum, and the potential barrier is 19.7 kcal/mol. When the DFT-PBE method is used, the potential bar-

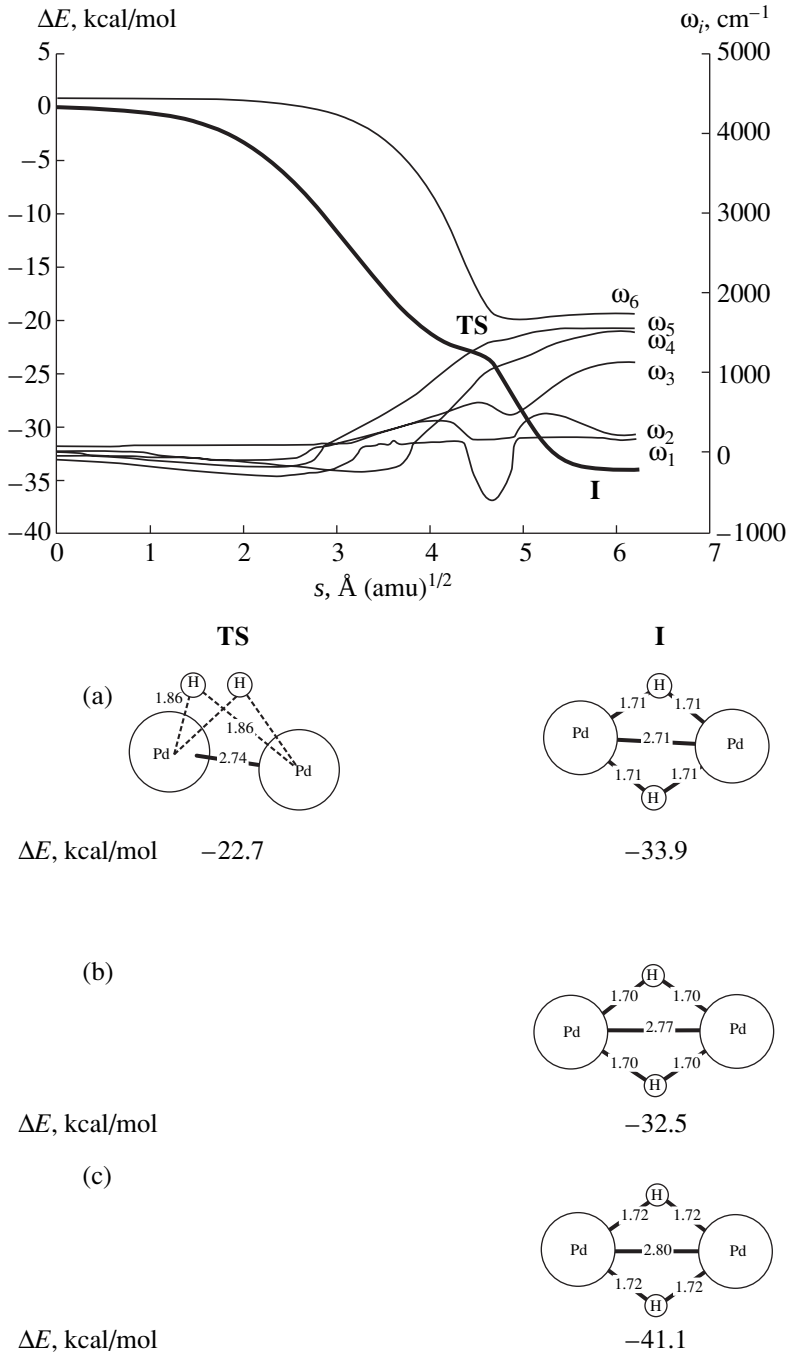


**Fig. 2.** Changes in the relative energy (thick line) ($\Delta E$) and normal vibratio§§§§§§§nal frequencies ($\omega_i$) along the reaction coordinate ($s$) for the oxidative addition of $H_2$ to $Pd_2$ ($RP_1$). Structures of stationary points calculated by (a) CNDO/$S^2$, (b) DFT-BLYP, and (c) DFT-PBE. Bond lengths are in Å.

rier is 28.2 kcal/mol and the energy of product **II** is 1.3 kcal/mol lower. Note that, in all stationary points calculated by CNDO/$S^2$ and DFT methods, the frequency $\omega_{1a}$ has a low imaginary value (~50i $cm^{-1}$). Thus, the *trans*-complex has one vibrational vector with a low imaginary value. A shift along this vector results in the translation of $Pd_2H_2$ and $C_2H_4$ toward each other.

### *$C_2H_4$ Addition to $Pd_2H_2$*

Motion along $RP_3$ results in a substantial decrease in energy (Fig. 4). $RP_3$ consists of two parts. One is gently sloping and corresponds to the coordination of the ethylene molecule on one palladium atom to form intermediate complex **III** with an energy decrease by 9.1 (CNDO/$S^2$), 9.3 (DFT-BLYP), or 10.8 kcal/mol

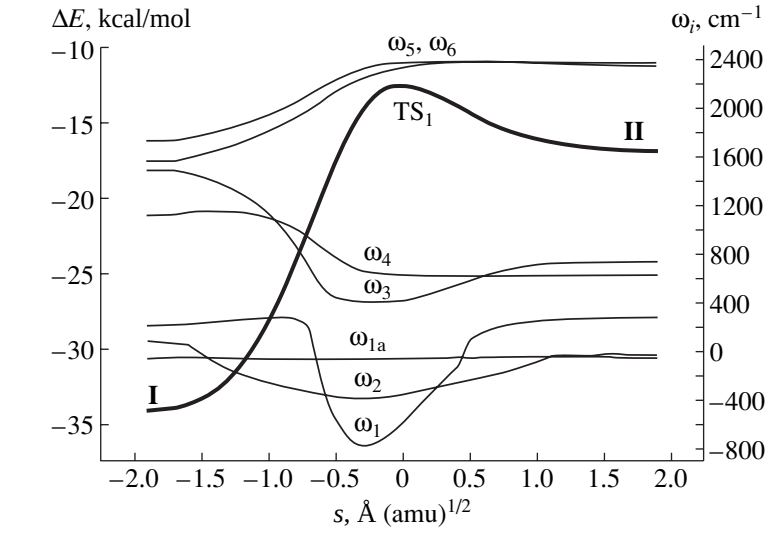


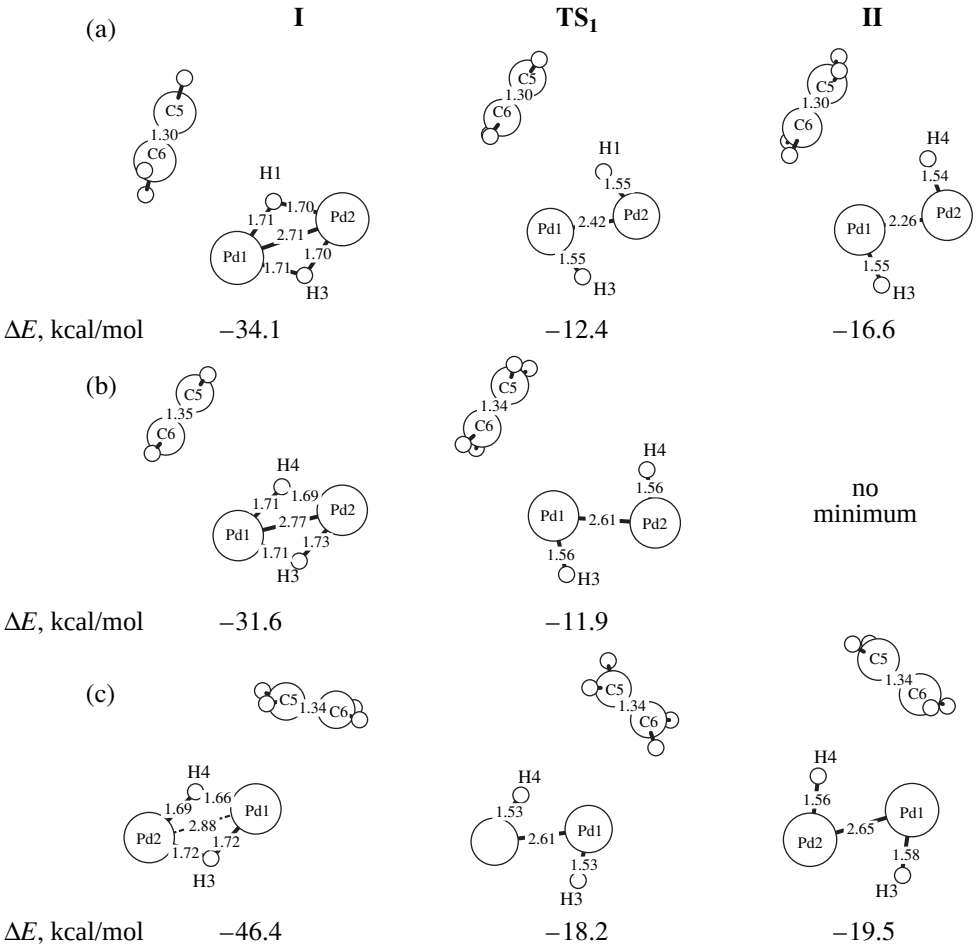


**Fig. 3.** Changes in the relative energy (thick line) ($\Delta E$) and normal vibrational frequencies ($\omega_i$) along the reaction coordinate (s) for $Pd_2H_2$ isomerization from pseudosquare (**I**) to *trans*-complex (**II**) ($RP_2$). Structures of stationary points calculated by (a) CNDO/$S^2$, (b) DFT-BLYP, and (c) DFT-PBE. Bond lengths are in Å.

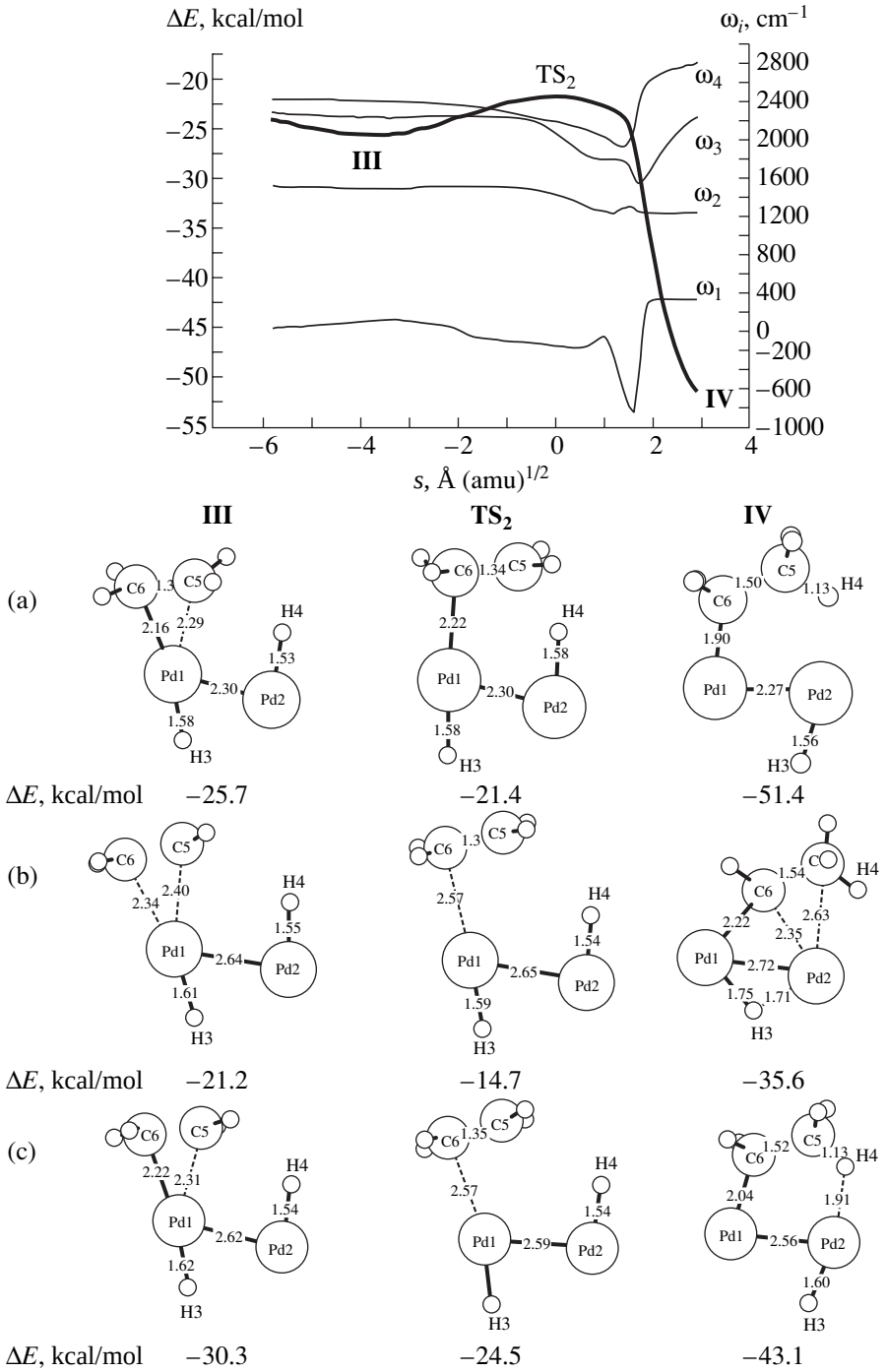


**Fig. 4.** Changes in the relative energy (thick line) ($\Delta E$) and some normal vibrational frequencies ($\omega_i$) along the reaction coordinate ($s$) for $C_2H_4$ addition to $Pd_2H_2$ ($RP_3$). Structures of stationary points calculated by (a) CNDO/$S^2$, (b) DFT-BLYP, and (c) DFT-PBE. Bond lengths are in Å.

(DFT-PBE) at a long segment of 9 Å $(amu)^{1/2}$. The other one is steeper; this part is associated with synchronous Pd–H bond breaking, C–H bond formation, and the transfer of one Pd atom to another. The second part of $RP_3$ includes transition state $TS_2$ with a barrier of 4.3 (CNDO/$S^2$), 6.5 (DFT-BLYP), or 5.8 kcal/mol (DFT-PBE) and a drastic decrease in the energy of product **IV** by 30.0 kcal/mol (CNDO/$S^2$), 20.9 (DFT-BLYP), or 18.6 kcal/mol (DFT-PBE). This is the *trans*-product of C–H bond activation in ethane (CNDO/$S^2$ and DFT-PBE) or a bridged product (DFT-BLYP). Figure 4 also shows four measured vibrational frequencies: $\omega_1$ corre-

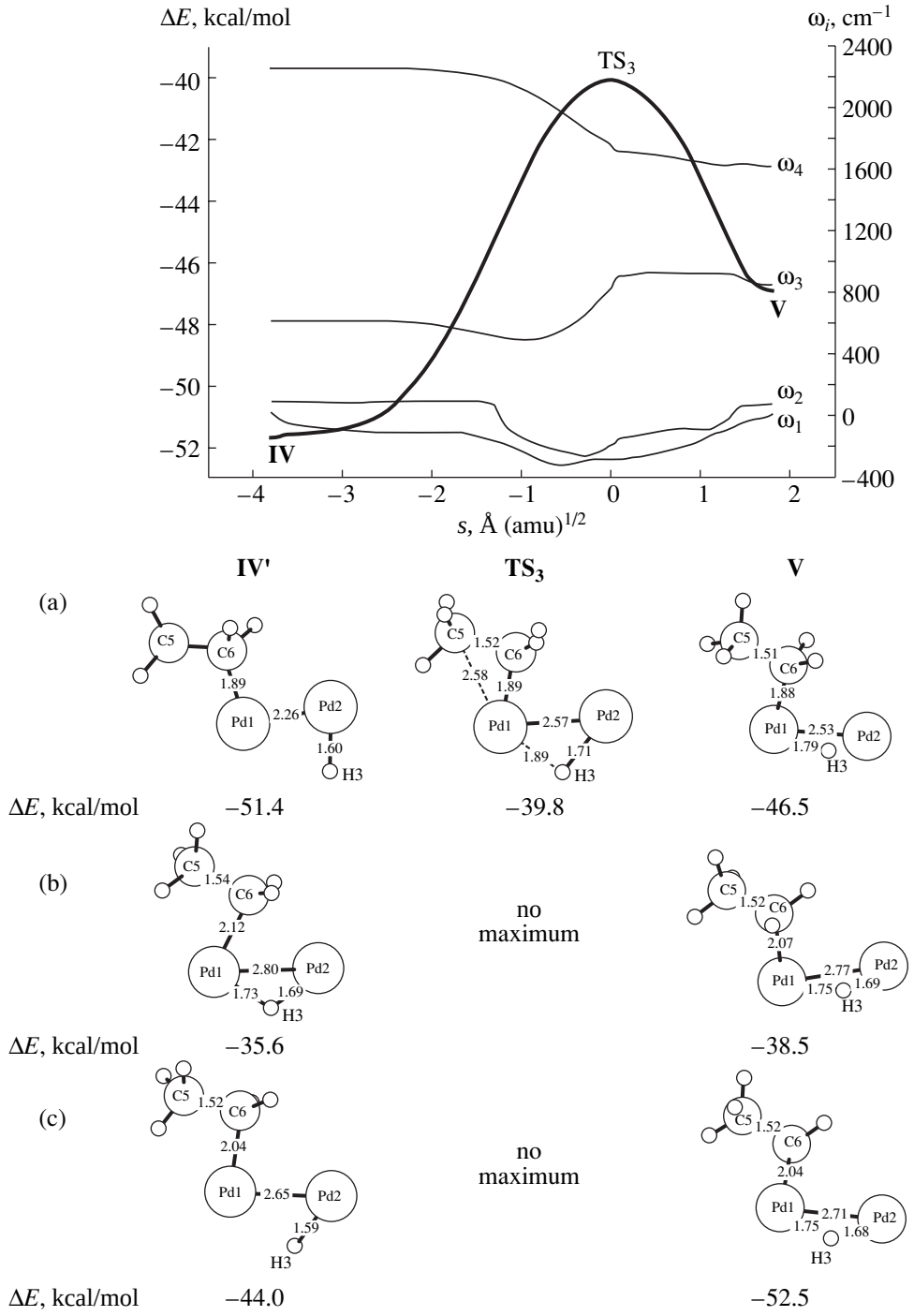


**Fig. 5.** Changes in the relative energy (thick line) ($\Delta E$) and some normal vibrational frequencies ($\omega_i$) along the reaction coordinate (*s*) the isomerization of the *trans*-product of C–H bond activation in ethane molecule (**IV'**) into bridged complex (V) ($RP_4$). Structures of stationary points calculated by (a) CNDO/$S^2$, (b) DFT-BLYP, and (c) DFT-PBE. Bond lengths are in Å.

sponds to the reaction coordinate; $\omega_2$ corresponds to C–C vibration, which changes from the value in ethylene to that in ethane; $\omega_3$ is the vibration of the Pd1–H3 bond, which first transforms into a bridging bond (Pd1–H3–Pd2) with a decrease in the frequency and then into the Pd2–H3 bond with an increase in frequency; $\omega_4$ corresponds to the vibration of the Pd2–H4 bond, which transforms into a C–H bond. Note that the CNDO/$S^2$ method overestimates the stability of the *trans*-product. The next area of the potential energy surface for the catalytic cycle is associated with a vibrational mode, which is analogous to $RP_1$.

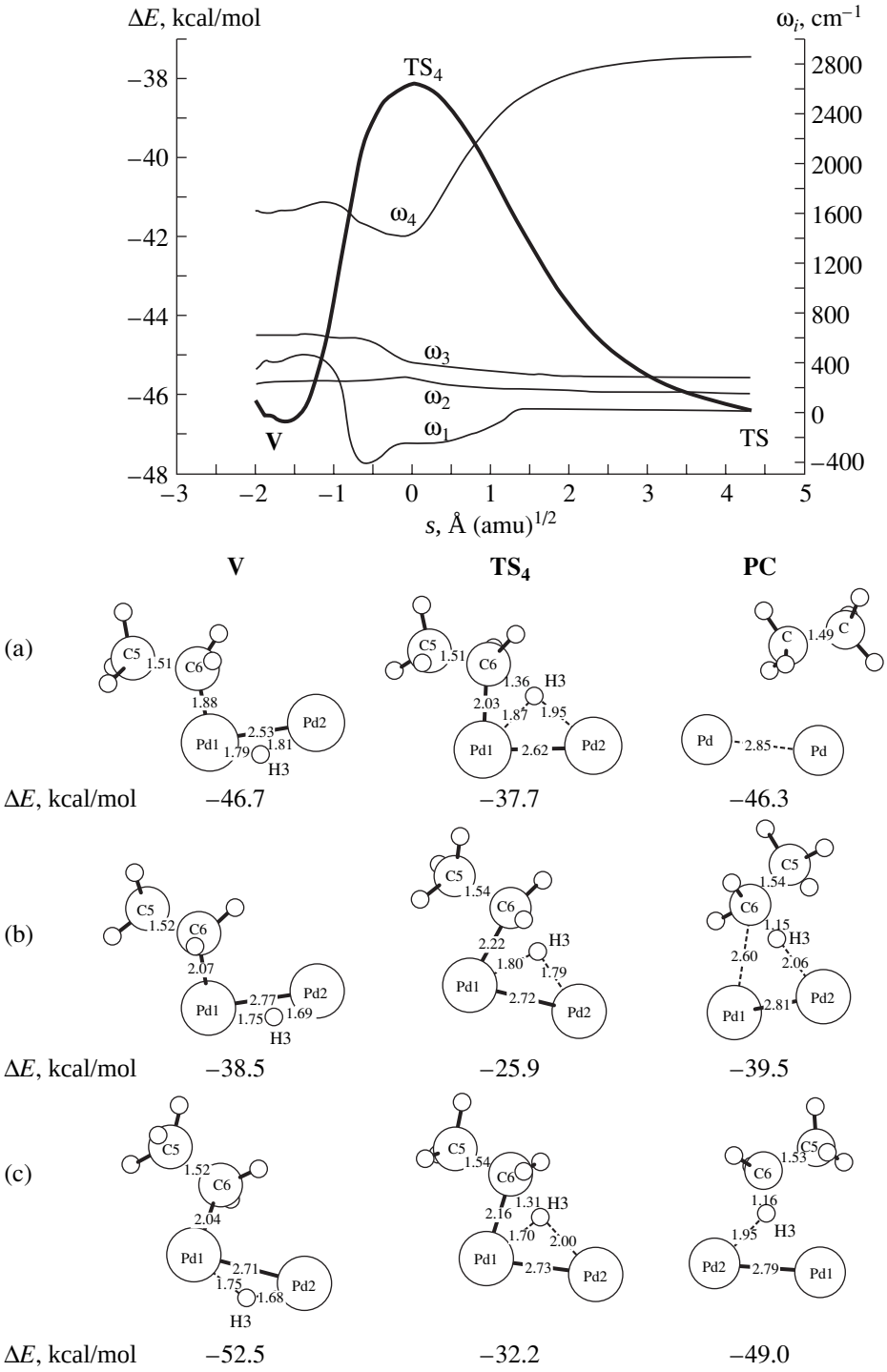


**Fig. 6.** Changes in the relative energy (thick line) ($\Delta E$) and some normal vibrational frequencies ($\omega_i$) along the reaction coordinate ($s$) for ethane reductive elimination ($RP_5$). Structures of stationary points calculated by (a) CNDO/S[2], (b) DFT-BLYP, and (c) DFT-PBE. Bond lengths are in Å.

### *$HPdPdC_2H_5$ Complex Isomerization*

A vector corresponding to $RP_4$ restructures *trans*-product **IV**' formed from **IV** by barrier-free rotation along the Pd–C bond. As a result, product **V** with a bridging Pd–H–Pd bond tilted to 90° relatively to the C–Pd–Pd plane is formed (Fig. 5). Product **V** is 4.7 kcal/mol higher than the *trans*-product. The barrier toward **V** ($TS_3$) is 11.6 kcal/mol with a width of

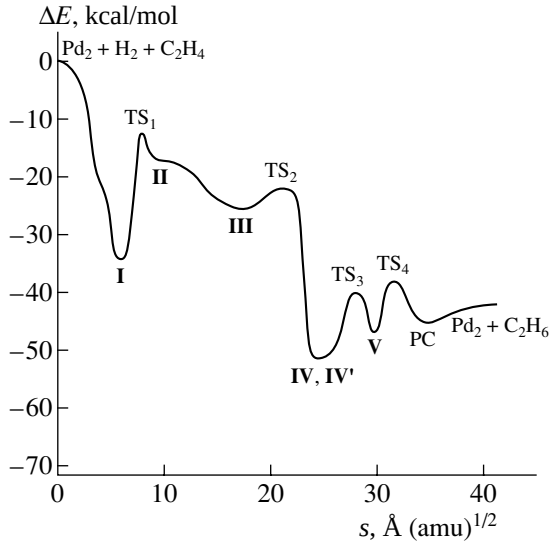


**Fig. 7.** Potential energy profile along the normal reaction coordinate *s* for reactions (I) and (II) of the catalytic cycle.

~4 Å $(amu)^{1/2}$. This barrier is an artifact of the CNDO/S[2] method, which overestimates the stability of products **IV** and **IV'**. According to DFT calculations, there is no any barrier in this process. The saddle point $TS_3$ has two imaginary frequencies $\omega_1$ and $\omega_2$. One leads to product **V**, and the other leads to **IV'**. Figure 5 also shows frequencies $\omega_3$ and $\omega_4$ associated with the vibrations of Pd–Pd–H and Pd–H, respectively. Product **V** has a vibrational mode resulting in the final step of the catalytic cycle, which is the reductive elimination of ethane.

### *Reductive Elimination of Ethane*

Vector $RP_5$ includes the approach of proton H3 and C4 through the rotation along the Pd–Pd bond from product **V** to saddle point $TS_4$ with an increase in energy by 9.4 kcal/mol (Fig. 6). Then, the bridging Pd–H–Pd bond breaks in $TS_4$ synchronously with the formation of a new C–H bond, which results in the formation of a pre-reaction complex (PC) of separate $Pd_2$ and $C_2H_6$ molecules, whose energy is 0.4 kcal/mol higher than in complex **V**. Figure 6 also shows changes in some frequencies along $RP_5$. Specifically, $\omega_4$ refers to transition from Pd–H vibration to C–H vibration.

## CONCLUSION

The complete catalytic cycle of ethylene hydrogenation with a dipalladium cluster consists of five consecutive steps. Figure 7 shows the potential that unites all reaction paths. The overall positive energetic effect is 42.6 kcal/mol.

Our results suggest that ethylene hydrogenation to ethane occurs via the formation of the *trans*-product ($RP_2$) from the pseudosquare complex ($RP_1$). The length of the activated H–H bond increases from ~2 to ~3 Å and ethylene is able to react only with one activated hydrogen atom ($RP_3$). $RP_3$ is the transformation of **III** into **IV** (Fig. 4). It is active because the potential barrier is low (~5 kcal/mol), and the energy of product **IV** is 15–25 kcal/mol lower than that of **III**.

The experimental study of ethylene hydrogenation by bulk hydrogen on Ni(111) [36] shows that hydrogen atoms that escape from the metal bulk onto the surface readily hydrogenate ethylene adsorbed on Ni(111) to form ethane. This corresponds to the activity of *trans*-reagent **II**. According to that experimental study, surface-bound hydrogen is inactive in hydrogenation, which is consistent with pseudosquare complex **I** inactivity.

The most efficient catalysts are probably bimetallic complexes that readily form *trans*-complexes by $H_2$ addition. The catalytic system based on transition-metal bimetallic clusters based on metalloporphyrin proposed in our earlier paper possesses this property [37].

## REFERENCES

1. Dedieu, A., *Inorg. Chem.*, 1981, vol. 20, no. 9, p. 2803.
2. Jolly, C.A. and Marynick, D.S., *J. Am. Chem. Soc.*, 1989, vol. 111, no. 20, p. 7968.
3. Kawamura-Kuribayashi, H., Koga, N., and Morokuma, K., *J. Am. Chem. Soc.*, 1992, vol. 114, no. 7, p. 2359.
4. Siegbahn, P.E.M., *J. Am. Chem. Soc.*, 1993, vol. 115, no. 13, p. 5803.
5. Koga, N., Obara, S., Kitaura, K., and Morokuma, K., *J. Am. Chem. Soc.*, 1985, vol. 107, no. 24, p. 7109.
6. Sargent, A.L. and Hall, M.B., *Inorg. Chem.*, 1992, vol. 31, no. 2, p. 317.
7. Sargent, A.L., Hall, M.B., and Cuest, M.F., *J. Am. Chem. Soc.*, 1992, vol. 114, no. 2, p. 517.
8. Sakaki, S. and Ikei, M., *J. Am. Chem. Soc.*, 1991, vol. 113, no. 13, p. 5063.
9. Sakaki, S. and Ikei, M., *J. Am. Chem. Soc.*, 1993, vol. 115, no. 6, p. 2373.
10. Koga, N. and Morokuma, K., *J. Am. Chem. Soc.*, 1993, vol. 115, no. 15, p. 6883.
11. Sakaki, S., Bismas, B., and Sugimoto, M., *Organometallics*, 1998, vol. 17, no. 7, p. 1278.
12. Avdeev, V.I. and Zhidomirov, G.M., *Kinet. Katal.*, 1996, vol. 37, no. 5, p. 775.
13. Clot, E. and Eisenstein, O., *J. Phys. Chem.*, 1998, vol. 102, no. 20, p. 3592.
14. Macgregor, S.A., Eisenstein, O., Whittlesey, M.K., *et al.*, *J. Chem. Soc., Dalton Trans.*, 1998, no. 2, p. 291.
15. Mamaev, V.M., Gloriozov, I.P., Ischenko, S.Ya., *et al.*, *J. Chem. Soc., Faraday Trans.*, 1995, vol. 91, no. 21, p. 3779.
16. Mamaev, V.M., Gloriozov, I.P., Prisyajnyuk, A.V., *et al.*, *Mendeleev Commun.*, 1996, no. 5, p. 203.
17. Mamaev, V.M., Prisyazhnyuk, A.V., Gloriozov, I.P., *et al.*, *Kinet. Katal.*, 1998, vol. 39, no. 2, p. 178.

18. Mamaev, V.M., Gloriozov, I.P., and Prisyajnyuk, A.V., *Mendeleev Commun.*, 1998, no. 2, p. 53.
19. Koga, N., Daniel, C., Han, J., *et al.*, *J. Am. Chem. Soc.*, 1987, vol. 109, no. 11, p. 3455; 1988, vol. 110, no. 2, p. 3773.
20. Musaev, D.G., Mebel, A.M., and Morokuma, K., *J. Am. Chem. Soc.*, 1994, vol. 116, no. 23, p. 10693.
21. Matsubara, T., Koga, N., Ding, Ya., *et al.*, *Organometallics*, 1997, vol. 16, no. 5, p. 1065.
22. Gui, Qi., Musaev, D.G., and Morokuma, K., *Organometallics*, 1997, vol. 16, no. 7, p. 1355.
23. Gui, Qi., Musaev, D.G., and Morokuma, K., *Organometallics*, 1998, vol. 17, no. 4, p. 742.
24. Albert, K., Gisdakis, Ph., and Rösch, N., *Organometallics*, 1998, vol. 17, no. 8, p. 1608.
25. Koga, N. and Morokuma, K., *Chem. Rev*, 1991, vol. 91, no. 5, p. 283; Niu, S. and Hall, B., *Chem. Rev.*, 2000, vol. 100, no. 2, p. 353; Torrent M., Solá, M., and Frenking, G., *Chem. Rev.*, 2000, vol. 100, no. 2, p. 439; Dedieu, A., *Chem. Rev.*, 2000, vol. 100, no. 2, p. 543.
26. Mamaev, V.M., Gloriozov, I.P., Siminyan, V.V., *et al.*, *Mendeleev Commun.*, 1997, no. 6, p. 246.
27. Miller, W.H., *J. Phys. Chem.*, 1983, vol. 87, no. 20, p. 3811.
28. Filatov, M.Yu., Gritsenko, O.V., and Zhidomirov, G.M., *Zh. Strukt. Khim.*, 1988, vol. 29, no. 3, p. 3.
29. Filatov, M.J., Gritsenko, O.V., and Zhidomirov, G.M., *J. Mol. Catal.*, 1989, vol. 54, no. 3, p. 452.
30. Nanda, D.N. and Jug, K., *Theor. Chim. Acta*, 1980, vol. 57, no. 2, p. 95.
31. Rusanov, V.V., Gloriozov, I.P., and Mamaev, V.M., *Zh. Strukt. Khim.*, 1993, vol. 34, no. 2, p. 170.
32. Becke, A.D., *Phys. Rev. A*, 1988, vol. 38, no. 6, p. 3098.
33. Lee, C., Yang, W., and Parr, R.G., *Phys. Rev. B*, 1988, vol. 37, no. 2, p. 785.
34. Perdew, J.P., Burke, K., and Ernzerhof, M., *Phys. Rev. Lett.*, 1996, vol. 77, no. 18, p. 3865.
35. Laikov, D.N., *Chem. Phys. Lett.*, 1997, vol. 281, no. 1, p. 151.
36. Daley, S.P., Utz, A.L., Trautman, T.R., *et al.*, *J. Am. Chem. Soc.*, 1994, vol. 116, no. 13, p. 6001.
37. Mamaev, V.M., Gloriozov, I.P., Lemenovskii, D.A., *et al.*, *Kinet. Katal.*, 2000, vol. 41, no. 1, p. 40.